

Non-contact one-sided evaluation of hidden corrosion in metallic constructions by using transient infrared thermography

V.P. Vavilov*

- Abstract** A short review of recent achievements in both theory and practice of transient infrared thermographic nondestructive evaluation in the application to corrosion detection is given. The potentials of 1D, 2D and 3D approaches to solving a heat conduction problem related to detecting material loss are compared, as well as the requirements to the inspection equipment are formulated. The practical illustrations are taken from the inspection of thin aluminum structures and thick steel samples.
- Keywords** Nondestructive evaluation of corrosion. Transient infrared thermography. Metallic construction inspection. Thermal detection theory. Detection of hidden corrosion.

Evaluación en una cara y sin contacto de la corrosión oculta en construcciones metálicas utilizando termografía infrarroja transitoria

- Resumen** Se presenta una corta revisión sobre los logros recientes en teoría y práctica de la evaluación no destructiva por termografía infrarroja transitoria aplicada a la detección de la corrosión. Se comparan los potenciales de las aproximaciones 1D, 2D y 3D para resolver el problema de la conducción del calor relacionada a la detección de pérdida de material, y, también, se formulan los requerimientos de los equipos de inspección. Se toman ilustraciones prácticas de la inspección de estructuras delgadas de aluminio y de muestras de acero gruesas.
- Palabras clave** Evaluación no destructiva de corrosión. Termografía infrarroja transitoria. Inspección de construcciones metálicas. Teoría de la detección del calor. Detección de corrosión oculta.

1. INTRODUCTION AND STATE-OF-THE-ART

Maintenance and repair of aging metallic constructions is a major concern in many industrial areas. Nondestructive evaluation (NDE) of corrosion is typically conducted by applying enhanced visual techniques, as well as using ultrasonic and eddy current inspection. Of course, potentials of visual inspection are rather limited when detecting hidden corrosion in a one-sided test procedure. Infrared (IR) thermography and laser shearography should be mentioned as relatively new techniques with limited industrial applications.

There are two main application areas for NDE methods: 1) detection of corrosion damage in aircraft aluminum fuselage lap joints, and 2)

detection of hidden corrosion in above-ground steel tanks. A comparative study of the off-the-shelf NDE equipment applied to locate and identify hidden corrosion damage on aircraft was recently performed in the U.S.A.^[1]. The six vendors demonstrated their NDE techniques by using samples of structures from retired aircraft. The conclusion about features of IR thermography was that this technique, although not a mature technology, may have some potentials and warrants further investigation.

The corrosion thermal detection theory is based on solving a differential equation of transient heat conduction in solids. In general case of small-size defects, this equation should be three-dimensional (3D) that typically requires using numerical methods. However, in many cases, reasonable

(*) Tomsk Polytechnic University, 634028, Tomsk, 28, Savinykh St., 3. Russia.

results can be obtained in a one-dimensional (1D) approximation. Basic features of transient temperature signals that evolve in defect areas were thoroughly discussed by Vavilov and Taylor in 1982^[2] and then by Vavilov in 1994^[3]. More specific works devoted to corrosion detection have appeared in the last decade^[4-18]. Vavilov *et al.* has shown that a solid sample with a buried defect is characterized with a specific heat transit time that is quite short in case of metals^[4]. Therefore, the corresponding inspection equipment should ensure a good time resolution in both heating and data acquisition. For example, in case of thin aluminum structures, such characteristic time may drop up to tens millisecond thus interfering with temperature scanning technique^[5]. Vavilov *et al.* has demonstrated that a robust inversion algorithm can be derived by analyzing a 1D simple adiabatic heat conduction solution^[4,7 and 8].

The most successful experimental realizations of corrosion detection in aerospace structures by transient IR thermography have been achieved by using flash tubes for heating a sample in the area of up to 0.5 m in diameter^[9-12]. A typical flash duration between 3 and 10 ms enables an accepted time resolution even in the inspection of thin aluminum^[10]. Some other types of thermal excitation, such as step-function (in time) and moving-line (in space), heating techniques have been proposed with a limited success due to the fact that in such case it is difficult to ensure a needed amount of absorbed heat energy for a short time^[14-16]. However, heating a sample with a moving heat line seems to be attractive presently because of a good spatial uniformity of heating and ease of practical implementation of this technique on site^[14]. In case of step-function heating, the problem is to subdue a back-reflected radiation that is achieved by irradiating a specimen with a laser operating at a wavelength out of spectral sensitivity of the IR imager^[15 and 16].

3D heat diffusion phenomena that occur in defect areas lead to shorter observation times and lower temperature signals that may be important in case of small-size defects^[7]. Almond *et al.* has shown that a temperature pattern over a buried defect shrinks in time thus distorting presentation of defect true dimensions^[13].

The most important problem when inspecting metals, in particular, glossy ones, is low absorbed energy and spurious reflections that causes a high level of false alarm. Partially, the latter effect can be reduced by using a dual-wavelength technique

that allows making both maps of temperature and emissivity^[17]. Another means to reduce noise is treating signals in time or phase domain. Such approach is becoming popular nowadays being implemented in dynamic thermal tomography^[3 and 7], time-resolved IR radiometry^[15 and 16] and pulse phase thermography^[18].

To summarize this short review of the state-of-the-art in the area of corrosion thermal NDE, it is worth noticing that the most successful studies have been conducted in the inspection of thin aluminum sheets. A very few works have dealt with the inspection of steel samples of up to 15 mm thickness^[8]. This is explained with the fact that thick steel samples require a large amount of absorbed energy that is hard to realize with available flash tubes.

2. THEORY

Corrosion damage can be modeled with a wall thinning which contacts with ambient or is filled with rust, paint etc. (see Fig. 1a). In both cases, this can be modeled with a simple plane geometry shown in figure 1b.

For practical reasons we shall consider only one-sided inspection procedures. It is obvious that a material layer over a defect will warm up faster than surrounding during heating and, oppositely, it will cool down faster in a cooling stage.

2.1. 1D approach

A 1D approach assumes that thermal events are so fast that lateral heat diffusion is negligible. Then, heat conduction in defect areas occurs independently on a sound area, i.e. edge effects are negligible. Thus, a defect area can be modeled with a three-layer plate shown in figure 2a. Respectively, a sound area is represented with a one-layer plate.

Solutions in non-defect areas are classical (see the 'bible' of heat conduction by Carslaw and Jaeger^[19]). Three-layer solutions are quite bulky even in simplified forms and not discussed here. The reader who is interested in the evident forms of these solutions is referred to^[20 and 21]. One of frequently used approximations for heat conduction in a three-layer plate (Fig. 2a) is that a central layer is characterized either with its thermal resistance or reflection coefficient^[20 and 22].

When detecting corrosion in metals, it can be assumed that heat does not propagate into a central layer being accumulated in the first layer. Hence, a

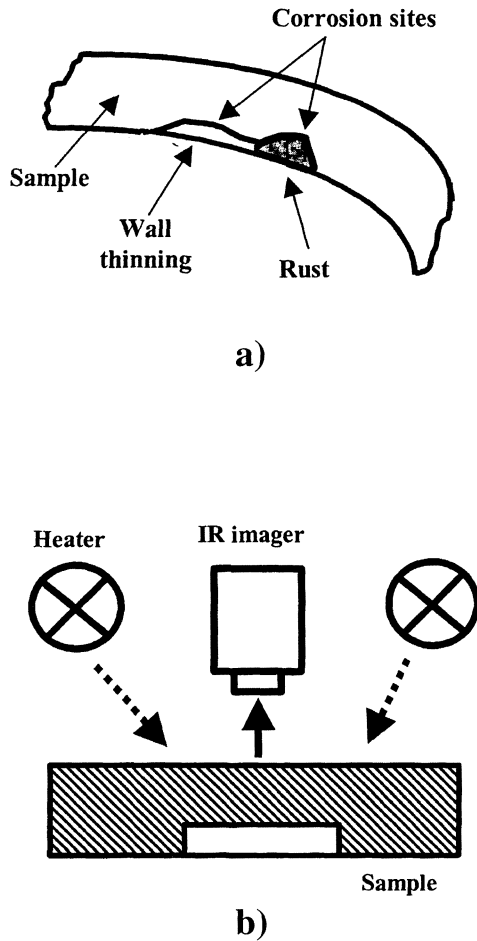


Figure 1. Modeling corrosion sites.

Figura 1. Modelización de los sitios de corrosión.

defect area can be modeled with a single plate of the remained thickness l that is to be confronted to a sound plate of thickness L (Fig. 2b).

To illustrate basic features of heat conduction in a corroded plate, we shall shortly discuss the well-known solution for a single adiabatic plate heated with a Dirac pulse (flash):

$$T_{nd}(z=0, \tau) = \frac{W\alpha}{KL} \left[1 + 2 \sum_{n=1}^{\infty} \exp(-n^2 \pi^2 Fo) \right] \quad (1)$$

Here $T(z, \tau)$ is the temperature on a heated surface; W is the absorbed energy (zero pulse duration); α is the sample thermal diffusivity; K is the sample thermal conductivity; L is the sample thickness, and $Fo = \alpha \tau / L^2$ is the Fourier number (dimensionless time). It is clear that in a stationary regime $T_{nd} = W\alpha / KL$.

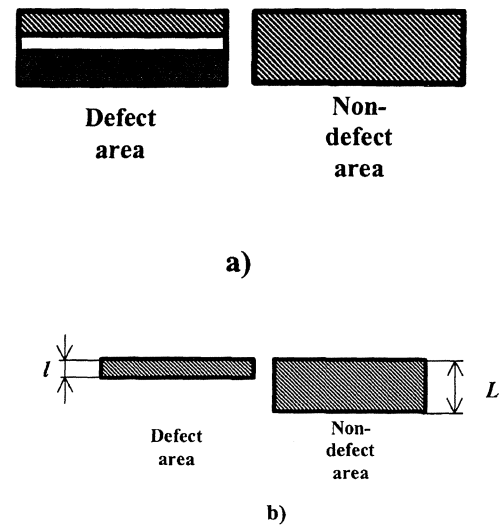


Figure 2. 1D approximation of defect and non-defect areas.

Figura 2. Aproximación 1D de las áreas defectuosas y no defectuosas.

For the sake of space we shall not discuss here heating a plate with a square pulse of τ_h duration. There is a simple approximation for the ratio between the temperature at the end of such a pulse and the stationary temperature:

$$m = T(z=0, \tau = \tau_h) / T(z=0, \tau = \infty) = 1.133 / \sqrt{Fo_h} \quad (2)$$

where $Fo_h = \alpha \tau_h / L^2$.

In a defect area, equation (1) acquires the form:

$$T_d(z, \tau) = \frac{W\alpha}{KL} \frac{1}{1-M} \left[1 + 2 \sum_{n=1}^{\infty} \exp(-n^2 \pi^2 Fo / (1-M)^2) \right] \quad (3)$$

where,

$M = 1-l/L$ is the material loss, l is the remained wall thickness. A surface temperature difference between defect and non-defect areas is:

$$\Delta T(z=0, \tau) = T_d(z=0, \tau) - T_{nd}(z=0, \tau) \quad (4)$$

The graphics illustrating equations (1) and (4) are shown in figure 3. It is seen that, in the adiabatic regime, a maximum temperature signal ΔT occurs in the stationary stage of the thermal process where:

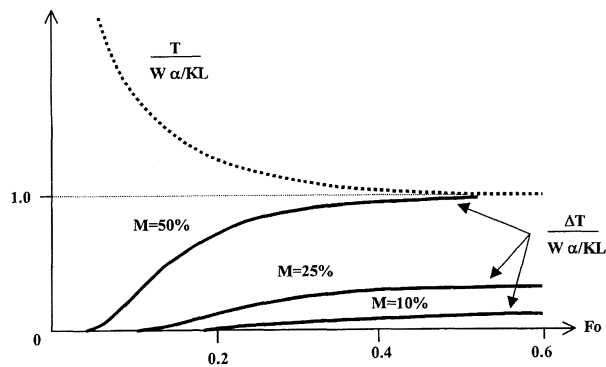


Figure 3. Evolution of temperature parameters vs. dimensionless time (M is the material loss).

Figura 3. Evolución de los parámetros de temperatura contra tiempo adimensional (M es la pérdida de material).

$$T_{nd}(z=0, \tau \rightarrow \infty) \rightarrow \frac{W\alpha}{KL}, T_d(z=0, \tau \rightarrow \infty) \rightarrow \frac{W\alpha}{Kl} \quad (5)$$

$$\Delta T_m(z=0, \tau \rightarrow \infty) \rightarrow \frac{W\alpha}{KL} \frac{M}{1-M} \text{ or } \Delta T_m(z=0, \tau \rightarrow \infty) \rightarrow \frac{W\alpha}{KL} \left(\frac{l}{l}-1\right)$$

2.1.1. Optimum observation time estimates

The best observation time τ_m is the time when $\Delta T(\tau)$ acquires the maximum value ΔT_m . In order to estimate τ_m , let us assume that this time arrives when the difference between the temperature and its stationary value becomes less than 1 % (the model by equation (1)). This gives $Fo_m \sim 0.54$. It is obvious that lateral heat exchange may change this time. For example, in thermal testing of buried defects, there is the following estimate of the best observation time: $\tau_m \sim l^2/\alpha$, where l is treated as the defect depth. Applying the last expression to corrosion detection produces $Fo_m \sim (l/L)^2 = (1-M)^2$. Verification of these estimates will be given below.

2.1.2. Corrosion detection limits

A corrosion site will be reliably detected if a temperature signal exceeds a noise level. Analysis of noise in thermal NDE is out of the scope of this paper. For simplicity sake, we shall assume that a temperature signal ΔT should match two conditions^[3]:

$$\Delta T(\tau_m) > \Delta T_{res} \text{ and } C_m = \Delta T(\tau_m)/T(\tau_m) > C_{noise} \quad (6)$$

where,

ΔT_{res} is the temperature resolution of the IR equipment, C_m is the dimensionless temperature

contrast, and C_{noise} is the noise contrast (the latter characterizes a particular sample surface).

The first condition in Eq.(6) determines the amount of energy that must be absorbed by a sample to ensure a reasonable temperature signal. For example, for 50 % corrosion ($M = 0.5$), it follows from equations (5) and (6) that:

$$W > KL\Delta T_{res} / \alpha. \quad (7)$$

Let us assume that $\Delta T_{res} = 0.1$ °C that is the typical value for commercial IR cameras. Then, detecting 50 % in a 2 mm aluminum sheet will require $W > 480 \text{ J/m}^2$ (thermal properties are taken from Table I). For a 10 mm AISI 316 steel sample, this value will increase up to $W > 3860 \text{ J/m}^2$. In practice, energy should be even more to ensure a reasonable temperature elevation above ambient for reliable detection. The consideration above might produce the impression that detection limit can be significantly enhanced by simple increasing absorbed energy, since in this case the only limit will be put by material destruction. Unfortunately, this is not absolutely true because of noise that increases with excess sample temperature.

Thus, a real detection limit is put by surface noise (rust, dust, paint, scratch etc.). From our previous experience, we found that, even on black-painted surfaces, the minimum noise is about $C_{noise} \approx 2$ %. By using equation (5) and the second condition from equation (6), we can obtain that the detection limit is $M_{min} \approx 2$ %. If to assume that a typical signal-to-noise ratio is about 3, the practical corrosion detection limit is about 5-6 % by material loss.

2.1.3. Example

Let us evaluate detection parameters for inspecting 25 % corrosion ($M = 0.25$) in a 10 mm AISI 1010 steel sample. We assume that the absorbed energy is $W = 15000 \text{ J/m}^2$ delivered in a 10 ms flash that is

Table I. Thermal properties of some metals

Tabla I. Propiedades térmicas de algunos metales

Metal	$K, W/(mK)$	$\alpha, 10^{-6} \text{ m}^2/\text{s}$
Steel AISI 316	13.4	3.47
Titanium	21.9	9.32
Steel AISI 1010	63.9	18.8
Aluminum alloy 2024-T6	177	73.0
Copper	365	100

high but practically achievable value. The stationary surface temperature is $T_{nd}(\tau=\infty) = 0.44$ °C and the temperature signal will be $\Delta T(\tau=\infty) = 0.15$ °C, see equations (1) and (5). Since $F_{oh} = 0.00188$ and $m = 26.3$, see equation (2), the temperature at the end of heating will be $\Delta T(\tau = \tau_h) = 11.6$ °C. The temperature contrast $C = \Delta T/T = 0.15/0.44 = 0.34$ is quite high but a temperature signal is rather low even for such high absorbed energy. Thus, this example illustrates the difficulty of heating a thick metal with a short pulse.

As for the optimum observation time, both estimates above give $F_{om} \sim 0.5$ that means $\tau_m \sim 2.7$ s.

More realistic estimates of the detection parameters will be given in case of a 2D and 3D geometry.

2.1.4. Quantitative evaluation of corrosion

The simplest inversion formula follows from equation (5) (see also [4,7 and 8]):

$$\frac{\Delta L}{L} = \frac{\Delta T/T}{1 + \Delta T/T} \quad (8)$$

For corroded areas of large lateral size, Eq.(8) is able to produce accuracy of few percent when operating at the best observation time^[4]. Its disadvantage is that a reference (non-defect) point is needed to determine ΔT . Therefore, an experimental procedure of corrosion detection involves identifying a suspicious area by the operator, then placing a reference point and, finally, estimating corrosion by equation (8).

2.2. 2D approach

The typical 2D geometries are Cartesian and cylindrical.

In Cartesian coordinates, a defect is simulated with a slot which is infinite in one coordinate direction (see Fig. 4a). For the same test conditions as described in the *Example* above, the 2D ΔT evolution is shown in figure 4b with the thin solid line (1D evolution calculated by equation (5) is presented with the dashed line). The maximum 2D temperature signal $\Delta T_m = 0.055$ °C occurs at the best observation time $\tau_m = 2.0$ s ($F_{om} = 0.38$, $C = 11.8$ %). Notice that the maximum 2D signal is about 3 times lower and occurs earlier than the corresponding 1D signal. Unlike the 1D approach, where temperature signals in defect and non-defect areas do not affect each other (see the dashed line

in figure 4c), a 2D spatial profile is Gaussian-like because it takes into account lateral heat diffusion by one coordinate (see the thin solid line in figure 4b). The example of the computed thermogram is shown in figure 4d). All computations have been performed by using Thermo.Heat-3D software from Tomsk Polytechnic University.

In cylindrical coordinates ('disk in disk' geometry), a defect is of finite size by all coordinates but it is azimuthally-symmetric. This geometry is often regarded as a good compromise between 1D and 3D situations (see details in^[3]).

2.3. 3D approach

Within a 3D approach, it is possible to simulate a defect of any size and shape by applying a relevant spatial grid. This situation is also illustrated with the data in figure 4 for the parallelepiped-like defect. The time evolution and the spatial distribution of the temperature signal are shown in figures 4b and 4c with the thick solid lines. It is clearly seen that lateral heat diffusion further reduces both the temperature signal and the time of its optimal observation (in the 3D case $\Delta T_m = 0.032$ °C at $\tau_m = 1.5$ s ; respectively $F_{om} = 0.3$ and $C = 6.4$ %). The IR thermogram for the 3D defect is shown in figure 4d.

The theoretical analysis above demonstrates that 25 % corrosion sites by size 10×10 mm in a 10 mm steel samples can be hardly detected by using available heaters and IR cameras due to very low signal amplitudes.

3. EQUIPMENT

3.1. Aerospace aluminum structures

To realize potentials of transient IR thermography in detecting hidden corrosion, the test equipment should exhibit some features that became recently available on the market^[23].

First of all, a heater must deliver a bunch of energy for a short period of time that must be shorter than expected observation times. Heat energy must be powerful enough to warm up a sample surface, at least, up to few centigrade above ambient. The reflected energy should be low to reduce noise. The features above can be achieved by using a set of flash tubes each of which typically supplies about 3 kJ for 5-10 ms. However, an inspected surface should be usually painted to enhance absorptivity and reduce noise.

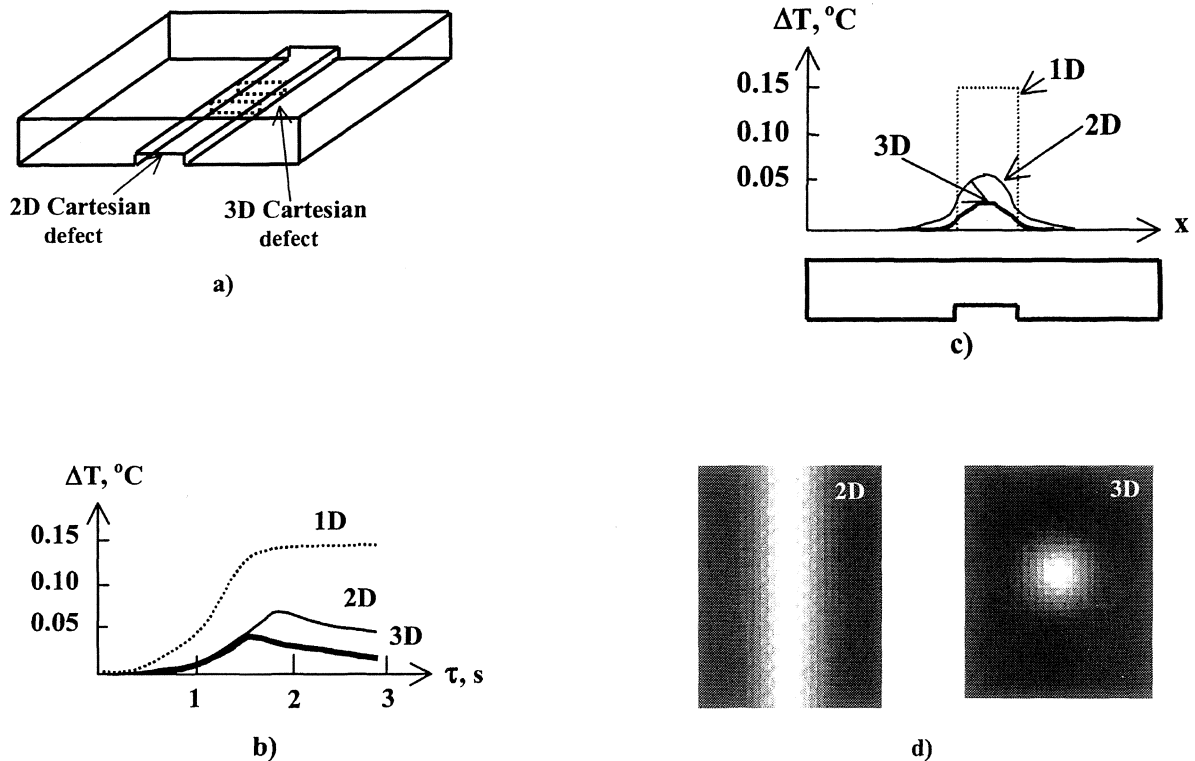


Figure 4. Detecting 25 % corrosion in a 10 mm AISI 1010 steel plate (defect lateral size 10 mm, heat pulse duration 10 ms, absorbed energy 15 kJ/m²): a) model, b) temperature signal vs. time, c) temperature signal vs. space, d) 2D and 3D temperature images at the best observation times.

Figura 4. Detección del 25 % de corrosión en una lámina de acero AISI 1010 de 10 mm (tamaño lateral del defecto 10 mm, duración del pulso de calor 10 ms, energía absorbida 15 kJ/m²): a) modelo, b) señal de temperatura contra tiempo, c) señal de temperatura vs. espacio, d) imágenes de temperatura 2D y 3D en los mejores tiempos de observación.

An IR acquisition system must ensure a proper time resolution (tens millisecond). This is easily achieved with modern focal plane array IR imagers operating in a snap-shot mode where all image pixels are viewed at one time. Frame frequency of such cameras can reach few hundred Hz.

3.2. Steel tanks

As the theory above showed, thick steel samples can be hardly stimulated with short heat pulses. Therefore, in this case, flash tubes should be replaced with quartz bulbs which allow smooth controlling of both power and pulse duration. The need of black painting remains valid also for thick metallic structures, such as above-ground tank, if these structures are not prior painted for technological reasons.

Since a time scale of thermal events in thick steel is much longer than in thin aluminum, IR

imagers can be relatively slow (even units with opto-mechanical scanning can be used).

In general, this application area still needs further research.

4. EXPERIMENTAL ILLUSTRATIONS

A lot of experimental illustrations can be found in [1,4,9-12,14,16 and 17]. Here we shall present a few illustrations to the inspection of both aircraft panels and thick steel samples.

Some panels of the D-8 aircraft were inspected thermographically (Fig. 5a). A black painted area of size about 40 cm was heated with two flash tubes. IR images were taken with an "Inframetrics-600" camera. The image in figure 5b exhibits rivets and four aluminum panels of 1 and 2 mm thickness (thinner aluminum sheets are hotter (Fig. 5b, see on the left).

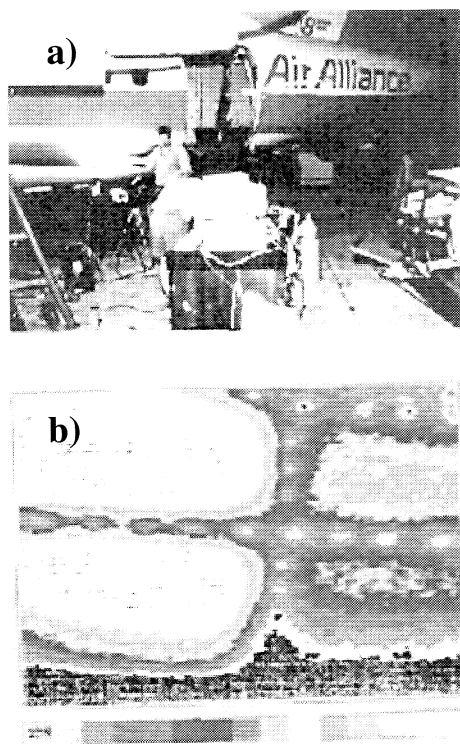


Figure 5. Inspecting aircraft aluminum panels at the airport of Quebec (courtesy of X.Maldague): a) inspection site, b) IR thermogram.

Figura 5. Inspección de los paneles de aluminio de un avión en el aeropuerto de Québec (cortesía de X. Maldague): a) sitio de inspección, b) termograma de IR.

The next illustration is presented in figure 6. A round-shaped 15 mm steel sample was heated with a set of tubular quartz bulbs for 300 s. IR thermograms were stored each 10 s by using "Thermovision-470" IR imager (140×140 pixel). Source images did not reveal any signs of the rear-surface defect that simulated 35 % corrosion except uneven heating patterns (Fig. 6a). After sophisticated data treatment by implying the algorithm of dynamic thermal tomography^[3 and 4], the round-shaped defect became quite visible (Fig. 6b). Notice that the original images in figures 5 and 6 are in color.

5. DATA PROCESSING ALGORITHMS

Description and comparison of data processing algorithms available in transient thermal NDT is beyond of the scope of this paper. We would like to state that importance of using a proper processing technique should not be underestimated, as illustrated by figure 6. The main purpose of data analysis is to enhance statistical parameters of defect detection by suppressing noise. The most

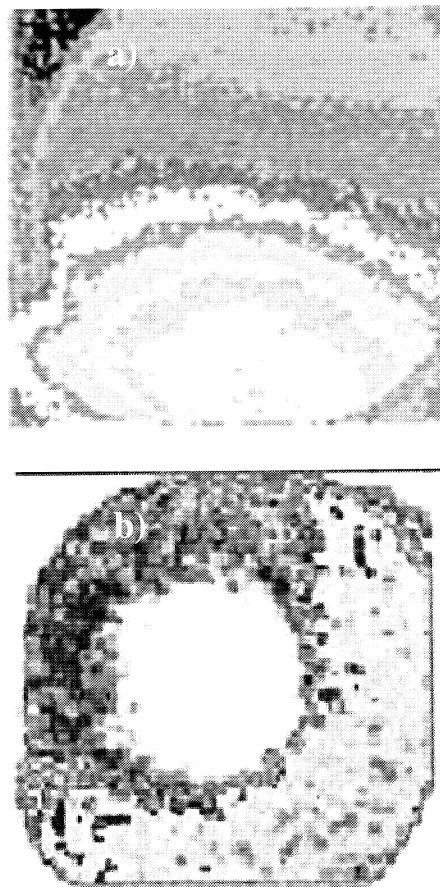


Figure 6. Evaluating 35 % corrosion in a 15 mm unpainted steel sample (delivering 1KW/m² for 300s): a) source image, b) thermal tomogram.

Figura 6. Evaluación del 35 % de corrosión en una muestra de acero no pintada de 15 mm (liberando 1KW/m² en 300 s): a) imagen de la fuente, b) termograma térmico.

promising algorithms are based on treating data in time or phase domain. The corresponding methodology can be found in^[3,9,10,12,14-18 and 22].

6. CONCLUSIONS

Inspection of corrosion in aluminum aircraft panels and above-ground steel tanks are the two main areas of application of transient IR thermography. However, these areas are rather different by the requirements to heating and recording equipment. Thin aluminum structures require delivering a short powerful pulse of thermal energy to resolve thermal events in a time range of tens millisecond. Focal plane array IR cameras operating in a snapshot mode are the most convenient to record such fast thermal events. A statistical detection limit can be of about few percent by material loss. In case of steel structures of 5-15 mm thickness, a

heating pulse should be optimized by energy and pulse duration to ensure a reasonable temperature elevation. Available 1D, 2D and 3D heat conduction theory allows such optimization. A detection limit in this case is estimated as about 20 % by material loss with the detection limit being put by stimulation energy.

REFERENCES

- [1] J. ALCOTT, *Mater. Evaluation*, January (1994) 64-69.
- [2] V. VAVILOV and R. TAYLOR, *Techn. in NDT*, R.Sharpe (ed.), vol.5, Academic Press, London, U.K., 1982, pp. 239-280.
- [3] V. VAVILOV, In: *Infrared Methodology and Technology*, X. Maldague (ed.), Gordon & Breach Science Publisher, U.S.A., 1994, pp. 230-309.
- [4] V. VAVILOV, E. GRINZATO, P.G. BISON, S. MARINETTI and M. BALES, *Int. J. Heat Mass Transf.*, 39 (1996) 355-371.
- [5] V. VAVILOV, E. GRINZATO, P.G. BISON, and S. MARINETTI, *Proc. of Eurotherm Seminar 42 Quant. Infrared Thermography – QIRT'94*, D.Balageas, G.Busse and G.M.Carlomagno (eds.), Sorrento, Italy, 1994, pp. 44-52.
- [6] V. VAVILOV, *Short Course Notes, SPIE – The International Society for Optical Engineering*, 1999, p. 95.
- [7] E. GRINZATO and V. VAVILOV, *Rev. Gen. Therm.* 37 (1998) 669-679.
- [8] V. VAVILOV, V. SHIRYAEV and E. GRINZATO, *Insight* 40 (1998) 408-410.
- [9] D.G. DAVID, J.Y. MARIN and H.R. TRETOUT, *Proc. SPIE “Thermosense-XIV”*, vol. 1682, Orlando, U.S.A., 1992, pp. 182-193.
- [10] X. HAN, L.D. FAVRO, T. AHMED, Z. OUYANG, L. WANG, X. WANG, P.K. KUO and R.L. THOMAS, *Rev. Progress in Quant. NDE*, vol. 17, D.O.Thompson and D.E.Chimenti (eds.), Plenum Press, N.Y., 1998, pp. 449-452.
- [11] A. DANIELS, *Proc. SPIE “Thermosense-XVIII”*, vol. 2766, 1966, pp. 185-201.
- [12] H.I. SYED, W. P. WINFREE, K.E. CRAMER and P. A. HOWELL, *Rev. Progress in Quant. NDE*, vol. 12, D. O. Thompson and D.E.Chimenti (eds.), Plenum Press, N.Y., 1993, pp. 1156-1161.
- [13] D.P. ALMOND, S. SAINTY and S.K. LAU, *Proc. Quant. Infr. Thermography QIRT'94*, Sorrento, Italy, pp. 247-252.
- [14] K.E. CRAMER and W.P. WINFREE, *Proc. SPIE “Thermosense-XX”*, vol. 3361, 1996, pp. 291-300.
- [15] R. OSIANDER and J.W.M. SPICER, *Rev. Generale Termique* 37 (1998) 680-692.
- [16] J.W.M. SPICER, *Rev. Progress in Quant. NDE*, vol. 12, D.O.Thompson and D.E.Chimenti (eds.), Plenum Press, N.Y., 1993, pp. 1149-1155.
- [17] N.K. DELGRANDE and P.F. DURBIN, *SPIE Optical Science, Engineering and Instrumentation Conference*, San Diego, U.S.A., 1995, p.10.
- [18] X. MALDAGUE and S. MARINETTI, *J. Appl. Phys.* 79 (1996) 2694-2698.
- [19] H.S. CARLSLAW and T.S. JAEGER, *Conduction of Heat in Solids*, Oxford University Press, Oxford, 1959.
- [20] D. BALAGEAS, J.C. KRAPEZ and P. CIELO, *J. Appl. Phys.* 59 (1986) 348-357.
- [21] A. DEGIOVANNI, *Int. J. Heat Mass Transfer* 31 (1988) 553-557 (in French).
- [22] L.C. AAMODT, J.W. MACLACHLAN and J.C. MURPHY, *J. Appl. Phys.* 68 (1990) 6087-6097.
- [23] J.J. SELMAN and J.T. MILLER, *Proc. SPIE “Thermosense-XV”*, vol. 1933, 1993, pp. 178-187.